A metal–organic framework *via* the reaction of benzoate with a cationic inorganic material†

Claudia H. Swanson, Steven P. Cummings, Martin Grysell, Dat T. Tran, David L. Rogow, Allen G. Oliver and Scott R. J. Oliver*

Received 30th June 2009, Accepted 9th September 2009
First published as an Advance Article on the web 30th September 2009
DOI: 10.1039/b912874c

Our research group previously reported a two-dimensional cationic inorganic material (BING-5, $Pb_3F_5NO_3$) where nitrate resides in the interlamellar space and can be anion exchanged. Investigation of the possible exchange of nitrate for benzoate led to the discovery of a layered metal–organic framework, lead benzoate hydrate $[Pb(C_6H_5CO_2)_2(OH_2)]$. The compound crystallizes as colourless plates in the monoclinic space group $P2_1/c$. The two dimensional lead–oxygen layers contain bridging benzoate oxygen atoms, with bridging water molecules further supporting the layers. The benzoate molecules are positioned perpendicular to the layers and form a hydrophobic bilayer region. The material shows basic character when immersed in various solvents suggesting potential as a base catalyst.

Introduction

Inorganic–organic hybrids[1] are a well studied class of materials with widespread application in areas such as catalysis[2-4] and hydrogen storage.[5-7] They are covalently extended structures containing metal atoms attached to organic ligands. Most inorganic–organic hybrid materials can be divided into two categories. Extended hybrids contain infinite metal–oxygen connectivity in one, two or three dimensions with organic molecules residing between the inorganic moieties. The second category represents metal–organic frameworks (MOFs), also known as coordination polymers, and can also be extended in one, two or three dimensions. The structural basis for this type of inorganic–organic framework is extended bonding between the metal centre and polyfunctional organic ligand. The range of ligands is enormous and can be varied to affect the desired geometry.[8,9]

There are several known MOFs, clusters and salts containing benzoate in the literature. The most notable examples are sodium and potassium benzoate due to their molecular nature and significance as preservatives in the food industry.[10,11] Benzoate anions form metal–organic clusters with a variety of elements: Mn,[12,13] Fe and Co,[14,15] Sb,[16] Cr,[17] Cu,[18,19] Ru,[20] Mo,[21] Bi,[22] Ca,[23,24] Li,[25] Sn,[26] Ag[27] and Zn.[28] Cobalt and calcium are the only current examples of benzoate MOFs, where hydrophobic bilayers of benzoate separate inorganic cobalt/calcium–oxygen layers. To date, there have been no examples of benzoate MOFs that include lead.

A cationic extended inorganic material previously reported by our research group, lead fluoride nitrate ($Pb_3F_5NO_3$, BING-5), contains $Pb_3F_5^+$ layers with nitrate in the interlamellar space.[29] The two-dimensional inorganic architecture consists of an inner neutral Pb_2F_4 layer capped by two outer positively charged $Pb_2F_3^+$ layers. Potential applications for BING-5 are catalysis due to its high temperature stability and wastewater treatment based on its anion exchange properties.[30-32] The initial publication of BING-5 indicates a successful exchange for dichromate anions, which raises the question whether the material is also suitable for exchange with other inorganic and organic anions. Proposed anions for potential exchange are monochromate, permanganate, perrhenate and benzoate.

Due to the interest of benzoate in daily life and the potential of $Pb_3F_5NO_3$ as an anion exchange material, the material was investigated for the possible uptake of benzoate. This paper analyzes in detail the reaction of lead fluoride nitrate with sodium benzoate. The attempted exchange resulted in the discovery of a crystalline metal–organic framework, lead benzoate hydrate. The crystal structure and properties of $Pb(C_6H_5CO_2)_2(OH_2)$ are discussed. The evolution of the crystal morphology is also followed by optical microscopy.

Results and discussion

The reaction of BING-5 ($Pb_3F_5NO_3$) and sodium benzoate was first performed in aqueous solution with a molar ratio of 1.0:1.5 for BING-5 to sodium benzoate. For the uptake of benzoate anions, the solution was examined by UV-Vis spectroscopy (Fig. 1). The absorption peak of sodium benzoate decreased over time, indicating that benzoate anions are disappearing from the solution. Optical micrographs in Fig. 2 confirmed the formation of new crystals on the surface of BING-5, the latter gradually disappearing by 18 h. To analyze the reaction for crystalline phase transformations, the progress of the reaction was also monitored by powder X-ray diffraction (PXRD). Fig. 3 shows the PXRD of the solid phase *versus* time. After 0.5 h, unknown peaks appear in the PXRD. The unknown crystalline phase shows maximum intensity after 4 h. The crystals from this time interval were manually separated and analyzed by single crystal X-ray diffraction (SCXRD).[20] A second unknown crystalline phase with a 2-Theta intensity at a lower angle also started forming after 0.5 h. This latter phase is the final product but could not be identified

---

Department of Chemistry and Biochemistry, 1156 High St., Santa Cruz, CA 95064, USA. E-mail: soliver@chemistry.ucsc.edu; Fax: +1(831)459-2935; Tel: +1(831)459-5448

† CCDC reference number 738466. For crystallographic data in CIF or other electronic format see DOI: 10.1039/b912874c

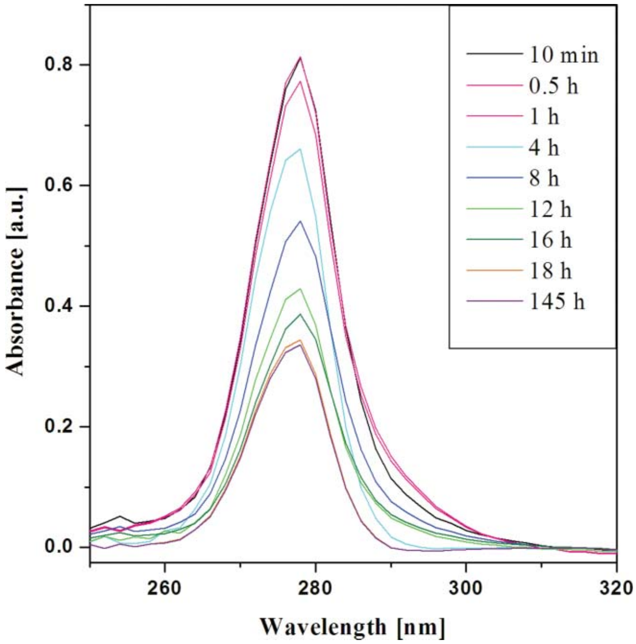

Fig. 1 UV-Vis spectroscopic measurements of the solution for the reaction of BING-5 with sodium benzoate. The benzoate absorption at $\lambda_{\max} = 280$ nm decreases over time.

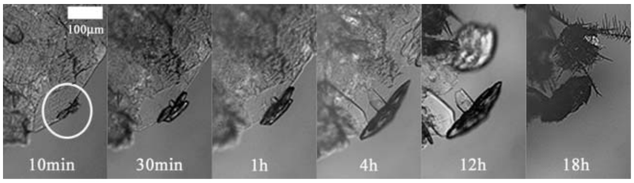

Fig. 2 Optical micrographs of the reaction of BING-5 with sodium benzoate solution. The first picture at 10 min shows the growth of crystals (white circled area) which gradually increases in size at the expense of the original BING-5 crystals. 10 min were required to allow the solution to settle and find a suitable imaging area.

due to the very small crystal size. Attempts at structure solution by refinement of PXRD data were not successful.

The first unknown crystalline phase was identified as lead benzoate hydrate, $Pb(C_6H_5CO_2)_2(OH_2)$. The structure will be abbreviated as SLUG-15 for University of California, Santa Cruz, structure number 15. The time frame for the presence of SLUG-15 in the PXRD pattern is from 10 min to 18 h. Characterization of only SLUG-15 initially could not be obtained since the compound co-crystallizes with the second unknown phase. Further experiments, however, were successful in obtaining phase-pure material.‡ Hydrothermal synthesis using lead(II) acetate and benzoic acid resulted in the identical crystalline structure, the large crystal size also allowing confirmation by SCXRD. The micrographs in Fig. 4 show the similarity of the crystal morphology from both syntheses. The characterization of SLUG-15 was performed using crystals from hydrothermal synthesis.

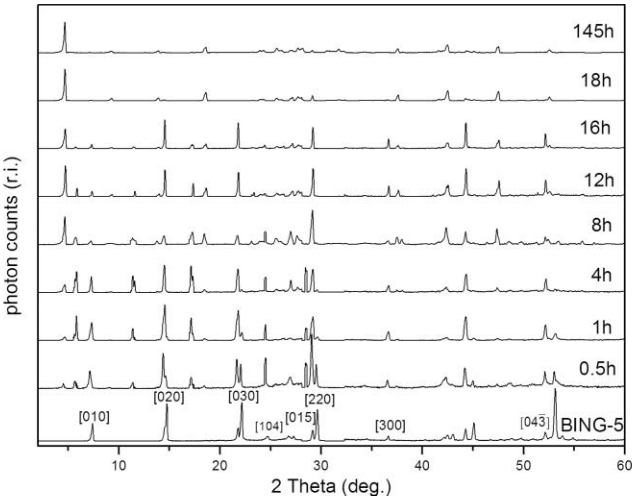

Fig. 3 *ex-situ* PXRD measurement *versus* reaction time of BING-5 with sodium benzoate. The main peak of SLUG-15 (5.7° 2θ) is present by 0.5 h, gradually declining in intensity to 16 h and finally absent after 18 h.

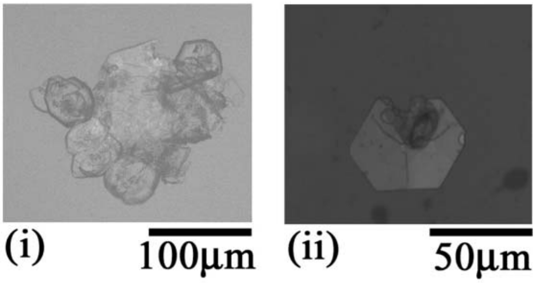

Fig. 4 Optical micrographs of SLUG-15 from: (i) reaction with BING-5 after 4 h reaction; (ii) hydrothermal synthesis.

SLUG-15 crystallizes as colourless thin plates from aqueous solution. There are four repeating asymmetric units in the unit cell in the monoclinic space group $P2_1/c$. The structure can be described as an extended solid of two-dimensional sheets of lead atoms bridged *via* the oxygen atoms of the benzoate ligands. The accepted range for a Pb–O covalent bond is *ca.* 2.2 to 2.5 Å,[33] while for an electrostatic interaction values can reach as large as 3.54 Å. The Pb–O bond lengths in SLUG-15 are 2.499(6) to 2.739(6) Å. One benzoate ligand coordinates to a lead centre *via* both oxygen atoms (η-2 coordination). The other benzoate has one oxygen atom coordinating in a bridging μ-2 configuration to two symmetry related lead atoms. The aromatic rings cap the surface of the sheets and form hydrophobic bilayers between the inorganic layers (Fig. 5). Within each monolayer, the benzoate molecules are arranged into pairs that pack into a grid-like array.

From the literature, a typical carbon–carbon bond distance in an aromatic benzene ring system is 1.39 Å. The values for the benzene rings in SLUG-15 are slightly different from the expected literature values. The C=C bond length varies between 1.376(13) and 1.402(15) Å. The carboxylate group is an electron withdrawing group, which likely causes the asymmetric form of the benzene ring. The literature bond length for a carboxylate C=O group is 1.27 Å, and the experimental values are 1.264(12) to 1.287(11) Å. The inorganic layer consists of 8-coordinated lead atoms bonded to water molecules and benzoate oxygen atoms

---

‡ Deionized water, lead(II) acetate and benzoic acid were added in a ratio of 100:1:1 [H_2O:$Pb(C_2H_5O_2)_2$:$C_6H_5CO_2H$, respectively] into a Teflon™-lined autoclave and treated for 3 days at 150 °C. The resultant crystals were isolated by filtration, rinsed with ethanol and dried at room temperature [yield: 98% (calculated from lead(II) acetate)].

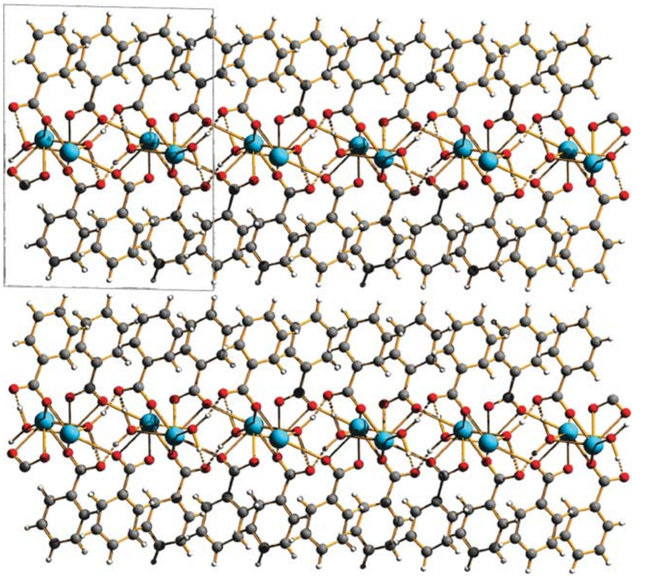

Fig. 5 *b*-projection of SLUG-15, showing the layers end-on. Colour scheme: Pb (light blue), O (red), C (grey) and H (white).

(Figs. 5, 6). The asymmetric unit consists of a lead(II) centre coordinated by two benzoate moieties and a μ-2 bridging water molecule (Fig. 7). The water molecule also forms hydrogen bonds to two nearby, symmetry-related benzoate oxygen atoms (O21) with nearly rhombohedral symmetry.

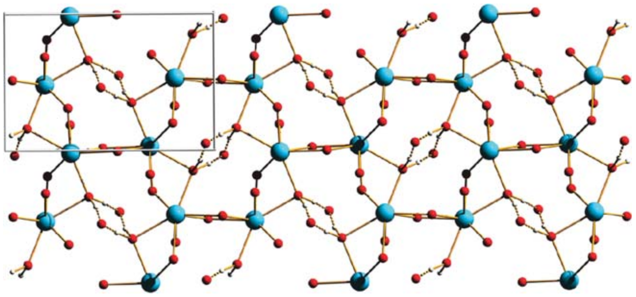

Fig. 6 *a*-projection of one layer, with carbon atoms omitted for clarity.

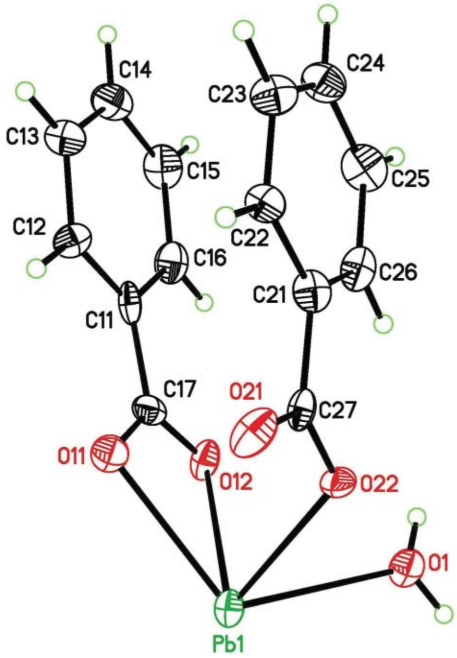

Fig. 7 ORTEP diagram of the asymmetric unit. Thermal ellipsoids calculated at 50% probability.

PXRD was investigated to confirm crystallinity and phase purity. Theoretical PXRD peaks agree well with the measured powder pattern (Fig. 8a-i). Elemental analysis percentages of carbon and hydrogen matched closely with the expected values (C: theor. 35.9%, exp. 35.1%; H: theor. 2.6%, exp. 2.1%). Thermogravimetric analysis (TGA) was performed to learn about stability and phase behaviour (Fig. 8b). The first weight loss before 100 °C of 3.7% corresponds to the loss of water (theor. 3.6%). This transition results in a highly amorphous powder with broad peaks in the PXRD pattern (Fig. 8a-iii) belonging to benzoate. The second and third weight losses of 26.6% (~ 275 °C) and 27.8% (~ 375 °C) correspond to the decomposition of one benzoate from the formula for each step (theor. 25.9% for each). The PXRD pattern after heating BING-5 *ex-situ* to 350 °C shows a mixture

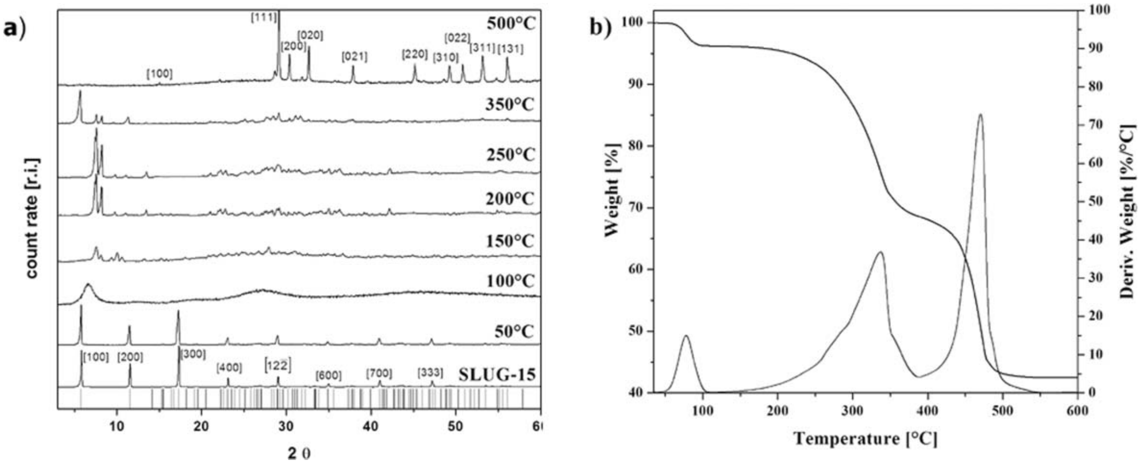

Fig. 8 (a) *ex-situ* PXRD patterns *versus* heating temperature in 50 °C steps to 250 °C [i–vi]; 350 °C [vii] and 500 °C [viii]. The theoretical PXRD pattern is illustrated with lines at the bottom. (b) TGA trace with first derivative shown.

of SLUG-15 and lead oxide. Lead oxide is the final product in the TGA above 500 °C, as confirmed by PXRD (Fig. 8a-viii).

Several other analytical techniques were employed to characterize SLUG-15. Differential scanning calorimetry (DSC) analysis shows an exothermic phase transition of 0.13 kJ g^{-1} at *ca.* 100 °C, which corresponds to the loss of water. ^1H NMR was employed to confirm the structure; all ^1H expected peaks for benzoate and bridging water molecules were found. IR spectroscopy confirmed the expected vibrations for the aromatic rings (1593, 1510, 701 cm^{-1}) and carboxylate groups (1400, 1068 cm^{-1}).

The properties of SLUG-15 in aqueous solution were analyzed to determine its acid/base strength. Therefore, 0.2 mmol of the material were added to 10 mL buffered solution. SLUG-15 shows good stability in pH 4 buffered solution but decomposes to lead(II) oxide in pH 7 or pH 10 buffered solution. When immersed in water without a buffer, the compound dissolves and releases benzoate, increasing the pH to 8.2. SLUG-15 also behaves as a base in organic solvents such as dichloromethane. In toluene, one of the most common solvents for organic synthesis, the material is stable and the pH increases from 5.5 to 10.3. The stability of SLUG-15 in both toluene and dichloromethane were confirmed by PXRD.

Experimental

BING-5 was synthesized hydrothermally according to published methods.[29] A ratio of 200:1:2 for H_2O:PbF_2:HNO_3 [deionized water, lead(II) fluoride (Acros, 99%) and nitric acid (Acros, conc. ACS reagent grade), respectively] were stirred for 30 min and heated at 150 °C for 3 days in a Teflon™-lined autoclave. The BING-5 crystals were separated, dried and characterized by powder X-ray diffraction (PXRD) to verify the product. 1.0 mmol BING-5 was then added to 1.5 mmol sodium benzoate (Alfa Aesar, 99%) dissolved in 50 mL distilled water and kept for 0.5–72 h in this solution. The mixture was monitored at various time intervals to follow the progress of the reaction. The filtered crystals from 4 h reaction time gave rise to lead(II) benzoate hydrate [estimated yield from PXRD peak ratio: 45%].

Instrumental

All products were initially characterized by PXRD with a Rigaku Americas Miniflex Plus powder diffractometer. Diffraction patterns were recorded from 2 to 60° 2θ, with a step size of 0.04° at 1°/min. For the temperature-dependent *ex-situ* measurements, the samples were placed in a crucible and heated in a Lindberg/Blue tube furnace to the desired temperature for 2 h. SCXRD (Table 1) was obtained on a Bruker APEX II CCD area detector X-ray diffractometer. Data was collected with $2\theta_{max}$ 28.61°, λ(Mo-Kα) 0.71073 Å and μ(Mo-Kα) 12.830 mm^{-1}. The observed data, $I > 2\sigma(I)$, were integrated by the program SAINT and analyzed for agreement and possible absorption using XPREP. An empirical absorption correction based on comparison of redundant and equivalent reflections was applied using SADABS. The structure was solved by direct methods and refined by full-matrix least-squares analysis of F^2 against all reflections. Programs used: Bruker APEX-2 v2.1; Bruker SHELXTL-Suite (v6.14); Diamond v3.1e (Crystal Impact, 2007).

Table 1 Crystal data and structure refinement for SLUG-15

empirical formula	$PbC_{14}O_5H_{12}$
formula weight [g mol^{-1}]	467.43
crystal system	monoclinic
space group	$P\,2_1/c$
a [Å]	15.411(2)
b [Å]	7.4635(12)
c [Å]	11.4497(18)
β [°]	91.279(2)
V [Å^3]	1316.6(4)
Z	4
temperature [K]	150(2)
$RI_1[I>2\sigma(I)]$	0.0517
wR_2 (all data)	0. 1288
Goodness of fit F^2	1.05
CCDC database no.	738466

TGA was measured on a TA Instruments 2050 TGA with nitrogen purge, heating from 30 to 600 °C at 10 °C/min and coupled to a mass spectrometer (Pfeiffer Vacuum, ThermoStar, GSD 301 T3) with a 70 eV ionizing potential. DSC was performed on a TA Instruments 2920 DSC using aluminium sample pans and a heating rate of 5 °C/min from 30 to 500 °C. Elemental analysis was performed by Quantitative Technologies, Inc. (Whitehouse, NJ). Infrared spectroscopy was completed on a SpectrumOne spectrometer from Perkin Elmer. NMR spectroscopy was carried out with a 600 MHz 5 mm Indirect Detection Probe and PFG (Pulse Field Gradients) in acetonitrile-d_3, CD_3CN. Scanning electron microscope (SEM) images were collected on a Hitachi S-2700 SEM. UV-Vis spectroscopy was performed on a Hewlett Packard HP-8452 spectrometer.

Conclusions

The anticipated anion exchange of nitrate for benzoate did not occur, instead yielding a 2-D MOF. We have nonetheless expanded the known MOFs of benzoate beyond Ca and Co. The double layers of benzoate create a hydrophobic bilayer. Further synthetic studies and/or refinement of powder data should allow a solution of the final unknown phase. The stability and basic character of the compound in both buffered aqueous solution and organic solvents suggest possible catalytic properties under mild conditions. Future studies include using other carboxylic acids as well as replacing lead for non-toxic elements such as bismuth and zinc.

Acknowledgements

This research was supported by an NSF Career Award (DMR-0506279). The single-crystal X-ray diffraction data in this work were recorded on an instrument supported by the NSF Major Research Instrumentation (MRI) program under grant no. CHE-0521569. We thank Jonathan Krupp at UC Santa Cruz for his help with the SEM micrographs. We also thank Alisyn Nedoma from Professor Balsara's group at UC Berkeley for help with DSC measurements.

Notes and references

1 A. K. Cheetham, C. N. R. Rao and R. K. Feller, *Chem. Commun.*, 2006, 4780–4795.
2 L. Alaerts, E. Seguin, H. Poelman, F. Thibault-Starzyk, P. A. Jacobs and D. E. De Vos, *Chem.–Eur. J.*, 2006, **12**, 7353–7363.

3 R. Evanhoe, *Chem. Eng. News*, 2006, **84**, 38–39.
4 X. D. Guo, G. S. Zhu, Z. Y. Li, F. X. Sun, Z. H. Yang and S. L. Qiu, *Chem. Commun.*, 2006, 3172–3174.
5 E. C. Spencer, J. A. K. Howard, G. J. McIntyre, J. L. C. Rowsell and O. M. Yaghi, *Chem. Commun.*, 2006, 278–280.
6 B. Xiao, P. S. Wheatley, X. B. Zhao, A. J. Fletcher, S. Fox, A. G. Rossi, I. L. Megson, S. Bordiga, L. Regli, K. M. Thomas and R. E. Morris, *J. Am. Chem. Soc.*, 2007, **129**, 1203–1209.
7 P. D. C. Dietzel, B. Panella, M. Hirscher, R. Blom and H. Fjellvag, *Chem. Commun.*, 2006, 959–961.
8 S. L. James, *Chem. Soc. Rev.*, 2003, **32**, 276–288.
9 Y. K. Park, S. B. Choi, H. Kim, K. Kim, B. H. Won, K. Choi, J. S. Choi, W. S. Ahn, N. Won, S. Kim, D. H. Jung, S. H. Choi, G. H. Kim, S. S. Cha, Y. H. Jhon, J. K. Yang and J. Kim, *Angew. Chem., Int. Ed.*, 2007, **46**, 8230–8233.
10 F. Sauer, *Special report – New York State Agricultural Experiment Station*, 1973, p. 22.
11 J. Chipley, *Food Sci. Technol.*, 1993, **57**, 11.
12 C. N. Chen, J. T. Chen, H. P. Zhu, Z. X. Huang and Q. T. Liu, *Sci. China, Ser. B: Chem.*, 2001, **44**, 320–327.
13 S. M. J. Aubin, Z. M. Sun, L. Pardi, J. Krzystek, K. Folting, L. C. Brunel, A. L. Rheingold, G. Christou and D. N. Hendrickson, *Inorg. Chem.*, 1999, **38**, 5329–5340.
14 M. Spohn and J. Strahle, *Z. Naturforsch., B: Chem. Sci.*, 1988, **43**, 540–546.
15 S. M. Gorun and S. J. Lippard, *Nature*, 1986, **319**, 666–668.
16 D. Rosmann, K. Hubler and A. Schmidt, *Monatsh. Chem.*, 1995, **126**, 1045–1050.
17 H. M. Gau and C. T. Chen, *Abstr. Pap. Am. Chem. Soc.*, 1992, **203**, 434-INOR.
18 T. Kawata, H. Uekusa, S. Ohba, T. Furukawa, T. Tokii, Y. Muto and M. Kato, *Acta Crystallogr., Sect. B: Struct. Sci.*, 1992, **48**, 253–261.
19 H. Koizumi, K. Osaki and T. Watanabe, *J. Phys. Soc. Jpn.*, 1963, **18**, 117.
20 M. Spohn, T. Vogt and J. Strahle, *Z. Naturforsch., B: Anorg. Chem. Org. Chem.*, 1986, **41**, 1373–1380.
21 F. A. Cotton, M. Extine and L. D. Gage, *Inorg. Chem.*, 1978, **17**, 172–176.
22 A. D. Rae, G. J. Gainsford and T. Kemmitt, *Acta Crystallogr., Sect. B: Struct. Sci.*, 1998, **54**, 438–442.
23 V. R. Cherkezova, F. N. Musaev and Z. S. Karaev, *Koord. Khim.*, 1987, **13**, 903.
24 I. Senkovska and U. Thewalt, *Acta Crystallogr., Sect. C: Cryst. Struct. Commun.*, 2005, **61**, m448–m449.
25 Stasova, *Kristallografiya (Russ.)*, 1959, **4**, 243.
26 M. M. Amini, S. H. Abadi, M. Mirzaee, T. Lugger, F. E. Hahn and S. W. Ng, *Acta Crystallogr., Sect. E: Struct. Rep. Online*, 2002, **58**, m697–M699.
27 M. Hedrich and H. Hartl, *Acta Crystallogr., Sect. C: Cryst. Struct. Commun.*, 1983, **39**, 533–536.
28 W. Clegg, D. R. Harbron and B. P. Straughan, *J. Crystallogr. Spectrosc. Res.*, 1990, **20**, 17–22.
29 D. T. Tran, P. Y. Zavalij and S. R. J. Oliver, *J. Am. Chem. Soc.*, 2002, **124**, 3966–3969.
30 A. Vaccari, *Appl. Clay Sci.*, 1999, **14**, 161–198.
31 J. Inacio, C. Taviot-Gueho, C. Forano and J. P. Besse, *Appl. Clay Sci.*, 2001, **18**, 255–264.
32 V. K. Gupta, I. Ali Suhas and V. K. Saini, *J. Colloid Interface Sci.*, 2006, **299**, 556–563.
33 P. Hewat, *Inorganic Crystal Structure Database (ICSD)*, Fachinformationszentrum Karlsruhe (FIZ), Karslruhe, Germany, 2007.